

MECHANICAL LINKS BETWEEN EROSION AND METAMORPHISM IN NANGA PARBAT, PAKISTAN HIMALAYA

P. O. KOONS*, P. K. ZEITLER**, C. P. CHAMBERLAIN***,
D. CRAW****, and A. S. MELTZER**

ABSTRACT. The mechanics and petrological signature of a collisional mountain belt can be significantly influenced by topographic and erosional effects at the scale of large river gorges. The geomorphic influence on crustal scale processes arises from the effects of both stress localization due to existing topography, and also erosional removal of advected crustal mass. The shear stress concentration and normal stress amplification due to topographic gradients and loads divert strain away from existing topographic loads, while concentrating strain into topographic gaps. Efficient erosional removal of material within topographic gaps with widths of at least the thickness of the brittle crustal layer results in differential advection of crustal material. Concentrated exhumation within a gap leads to thermal thinning of the upper brittle layer of the crust, removing the highest strength part of the continental crust and significantly reducing the integrated crustal strength beneath the topographic gap. A rheological weak spot, triggered by efficient incision, grows in intensity as strain becomes increasingly concentrated within the weak region. The growth of extreme topography of an isolated massif requires that the process of creation of the massif is related to the weakening process and can result from the velocity pattern produced by erosional-rheological coupling. As a result, distinctive thermal/mechanical regions develop within the crust in response to these river-influenced velocity patterns and these regions impose a characteristic signature on material advecting through. The signal is one in which the region of highest topography is bracketed by two high-strain zones between which concentrated advection produces lozenges of sillimanite and dry melt stability approximately 20 kilometers beneath the summit. Above these lozenges is a thermal/mechanical boundary layer containing an active hydrothermal system driven by steep thermal, topographic and mechanical gradients. These thermal mechanical regions are fixed with respect to a crustal reference frame. Passage of rock beneath and through these regions under these conditions produces the distinctive petrology and structure of mantled gneiss domes and is recorded within the moving petrological reference frame. Such erosional-rheological coupling can explain the occurrence of some high-grade gneiss domes in ancient collisional belts as well as the presence of active metamorphic massifs at both ends of the Himalayan orogen.

INTRODUCTION

One recent development in tectonics has been the recognition of the influence of topography and exhumation in controlling the metamorphic evolution of mountain belts (Pavlis and others, 1997; England and Thompson, 1984; Avouac and Burov, 1996). However, even when geodynamic models attempt to incorporate surface processes they fail to simulate the observed detailed distribution of metamorphic rocks. In particular, orogen-scale models incorporating orographic erosion patterns (Koons, 1990; Willett and others, 1993; Beaumont and others, 1996; Willett, 1999) do not predict the occurrence of high-grade culminations like gneiss domes associated with very large mountains. In fact, models conditioned by asymmetric orographic rainfall lead to predictions that the highest peaks in collisional orogens would consist

*Department of Geological Sciences, Global Sciences Center, University of Maine, Orono, Maine, 04469-5790, peter.koons@mail.maine.edu

**Department of Earth and Environmental Sciences, Lehigh University Bethlehem, Pennsylvania, 18015

***Department of Geological and Environmental Sciences Bldg. 320, Stanford University, Stanford, California, 94305

**** Department of Geology, University of Otago, Box 56, Dunedin, New Zealand

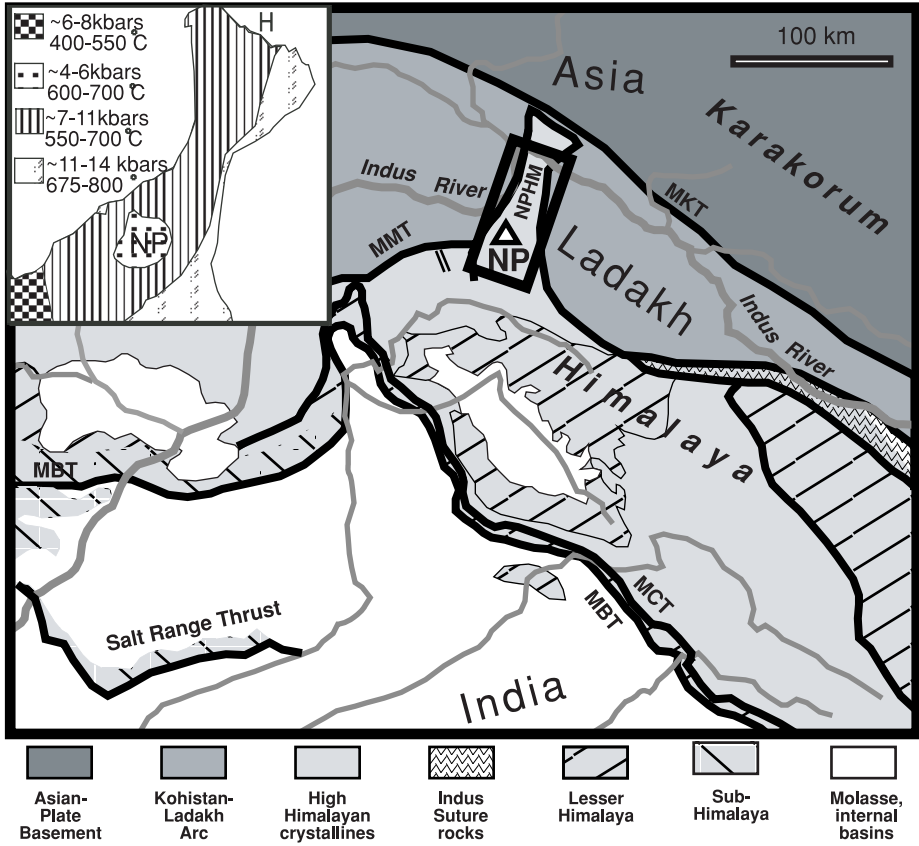


Fig. 1. Location of Nanga Parbat (NP)-Haramosh (H) Massif within the western Himalayan syntaxis. MMT = Main mantle thrust; MCT = Main central thrust; MBT = Main Boundary thrust; MKT = Karakorum fault. Inset shows domal metamorphic pattern with high temperature assemblages centered on Nanga Parbat massif summit surrounded by lower temperature, higher pressure assemblages (Poage and others, 2000; Zeitler and others, 2001a).

of upper crustal assemblages (Koons, 1990) while deep crustal assemblages would be restricted to lower elevations near the front of the orogens. The presence of crustal melts and granulites in several 8000-meter peaks of the Himalaya suggest incompleteness in mechanical models conditioned solely by orographic precipitation. Lithospheric buckling models have produced deep crustal upwelling (Burg and Podladchikov, 1999), but also produce massive upwards displacements of the Moho contrary to geophysical evidence (Park and Mackie, 2000; Meltzer and others, 2001).

In this paper, we investigate two issues: First, we examine the mechanical influence of geomorphic processes on strain patterns within a convergent orogen using simple analytical approximations of crustal strength. Second, we use a set of conditions suggested by field observations (Schneider and others, 1999a; Whittington and others, 2000; Zeitler and others, 2001a) on the evolution of the Nanga Parbat-Haramosh Massif (NPHM) in Northwest Pakistan (fig. 1) to model P/T implications imposed on metamorphic evolution by this mechanical model. The resulting mechanical model allows us to view an active orogen within the two reference frames used in classical studies: the instantaneous reference frame, fixed with respect to the crust, which pertains to electromagnetic and seismic observations; and the moving, material

reference frame which pertains to petrological observations that record, with only imperfect memory, the transit of rocks through the crustal frame.

Using a single mechanical framework to link the two sets of observations in active collisional orogens, we examine the local-scale evolution of the crust under the influence of the erosional, morphological, and mechanical state of the orogen, and discuss the petrological consequences for the evolution of rock/fluid packets that pass through this evolved crust. In brief, we find that erosional-rheological coupling, resulting from sustained fluvial incision into crust with a thermally-influenced shear resistance, can explain the development of characteristic metamorphic massifs in active orogens like Nanga Parbat and also Namche Barwa in the eastern Himalayan syntaxis. This coupling has significant implications for the formation of at least some high-grade gneiss domes in ancient orogens.

MODELING

The mechanical model used to simulate crust and assemblage evolution in high-grade metamorphic domes is conditioned by observations from NPHM. Geophysical and geological observations of NPHM are summarized elsewhere (Zeitler and others, 2001a), and those observations relevant to the mechanical modeling are:

1) Indian plate material of the NPHM antiform currently overthrusts Kohistan island-arc rocks from the south-southeast, with no evidence for tectonic exhumation or significant strike-slip faulting. Unlike the rest of the Himalayan front where southward-directed thrusting dominates, northward-directed shortening dominates only adjacent to deep gorges within the two Himalayan syntaxes, where the Indus in the west and the Tsangpo in the east (Gansser, 1964; Burg and others, 1997) slice across the Himalaya.

2) The 7000 meters of relief defined by Nanga Parbat and the Indus River reflect long-term erosional unroofing rates within the massif as high as 5 mm a^{-1} , and incision rates along the Indus as great as 12 mm a^{-1} (Burbank and others, 1996; Shroder and Bishop, 2000).

3) The topographic gap in the Kohistan Island Arc sequence defined by the NPHM bounded by the Indus, Astor and Gilgit valleys is currently between 25 and 50 kilometers.

4) The central core of the Nanga Parbat antiform exposes low-pressure granulite-facies gneisses; U-Pb ages of between 1 and 3 Ma from granites and migmatites in this central zone suggest 15 to 20 kilometers of unroofing in the past 3 Ma and granite emplacement during exhumation.

5) There is abundant evidence for elevated rock and fluid temperatures near the surface of the massif associated with extensive hydrothermal systems.

6) Strain is concentrated within the massif and at the boundaries with internal deformation accompanying the present exhumation (Kidd and others, 1998). The massif is not rising as a rigid block.

7) The distribution of microseismicity and fluid-inclusion evidence for an elevated geothermal gradient indicate shallowing of the ductile to brittle transition beneath Nanga Parbat to depths of ~ 5 to 8 kilometers beneath the surface (Meltzer and others, 2001).

8) Low seismic velocities centered under the Indus side of the summit massif extend to depth, and document that the local crust is hot, weak and ~ 40 kilometers thick (Meltzer and others, 2001). Magnetotelluric results show that the crust directly below the central NPHM is resistive and thus probably dry (Park and Mackie, 2000; Chamberlain and others, 2002).

MECHANICAL INFLUENCE OF TOPOGRAPHY AND EXHUMATION

In this section, we evaluate the influence of geomorphic components of topographic relief and exhumation on crustal strength and strain patterns. Influence of

geomorphic processes on the mechanical behavior of a deforming orogen can assume at least two forms, both related to the integrated strength of the crust (= F_c , Sonder and England, 1986). First, crustal strength may be perturbed by the differential loading by existing topographic features. Second, the process of exhumation can significantly influence the integrated strength of the crust through thermal weakening. In the discussion that follows, we examine perturbations due to these geomorphic effects on the approximation of crustal strength, with specific emphasis on the resulting strain effects.

Influence of Topography

In the following section, we assume that the region within the orogen being considered is at or close to failure in a convergent setting and therefore the discussion pertains to areas adjacent to the forethrust or backthrust with the minor principal stress, σ_3 , associated with the lithostatic normal stress ($\sigma_{zz} = \rho gh$). For simplicity, we assume a history of prior failure and choose a cohesionless ($S = 0$) material of friction angle, $\phi = 30^\circ$, giving a flow value, N , of 3, where N is defined as (Terzaghi, 1943):

$$N = \tan^2\left(\frac{\pi}{4} + \frac{\phi}{2}\right) = \frac{1 + \sin \phi}{1 - \sin \phi} \quad (1)$$

The value of the major compressive stress, σ_1 , as defined by

$$\sigma_1 = 2S\sqrt{N} + N\sigma_3 \quad (2)$$

produces a differential stress at failure of approximately twice σ_3 , for $\phi = 30^\circ$ ($\Delta\sigma = (\sigma_1 - \sigma_3) = \sigma_3(N - 1) = 2\sigma_3$). In an attempt to provide approximations of the geomorphic effect, we also assume a constant pore pressure ratio (Hubbert and Rubey, 1959), recognizing that an infinite variety of possible permutations of fluid pressure, rock compositions and strain-related rheologies may exist.

Unless the intermediate principal stress (σ_2) is close to the coordinate normal stress associated with either major or minor principal stresses, the topographic effect is generally insufficient to cause switching of the principal stresses and resultant displacement partitioning (Liu and Zoback, 1992; Enlow and Koons, 1998). For most of the examples considered here in this dominantly convergent part of the margin, the transition value of stress, $\hat{\tau}$, required to switch the sense of displacements from reverse to strike slip, given by:

$$\hat{\tau} = \sqrt{\tau_{xz}^2 + (\sigma_{xx} - \sigma_{yy})(\sigma_{yy} - \sigma_{zz})} \quad (3)$$

(Enlow and Koons, 1998) is not approached.

The influence of positive topographic loads on stress localization has been discussed elsewhere and arises from the combination of increased normal stress beneath the load, and shear stress concentration beneath the slopes and edges of the load (McTigue and Mei, 1981; Savage and Swolfs, 1986; Liu and Zoback, 1992; Enlow and Koons, 1998). The regional strain effects of a plateau-like topographic load, elongate ridge and isolated massif are similar in that each tends to deflect deformation away from the load to the region at the base of the confining slopes (England and Searle, 1986).

Negative topographic loads influence the shear and normal stress distribution in a similar manner (McTigue and Mei, 1981; Savage and Swolfs, 1986) and in this section, we concentrate on the influence of transverse valleys on regional strain. A four kilometer deep topographic gap through a mountain range, with a base width of the same dimension as the thickness of the brittle layer ($= \perp y$ in the reference frame of fig. 2) locally reduces the lithostatic normal stress, σ_{zz} , beneath the gap, and induces

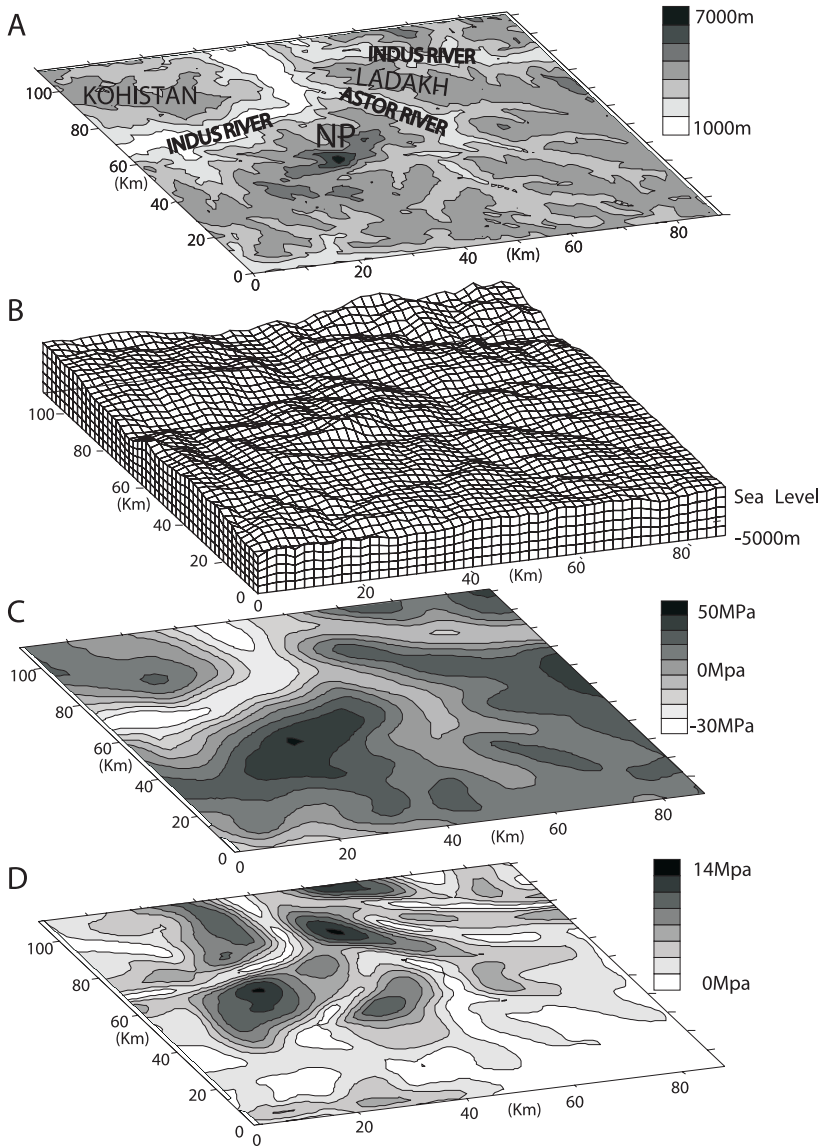


Fig. 2. Topography and topographically generated stresses within the NPHM and adjacent region. (A) Topography is derived by gridding GTOPO30 data at 878m x 1110 m intervals. Grid used for calculation of stress components. (B) Topography from 3a is imposed upon a 5 km thick grid of elastic/Mohr Coulomb material described in the text. (C) Topographic contribution to the vertical normal stress as represented by the departure of the vertical normal stress (σ_{zz}) at 5 km below sea level from that predicted by a constant 2 km elevation over the region. Maximum values correlate with elevation maxima and minima with the Indus and Astor valleys. (D) Vertical shear stress components $(\tau_{sxz}^2 + \tau_{syx}^2)^{1/2}$ generated by topography at 5 km below sea level. The maxima are sufficient to raise the differential stresses to near failure along the edge of the Nanga Parbat massif and the northern reaches of the Indus River.

vertical shear stress concentrations (τ_{iz}) beneath the valley slopes. Reduction of σ_{zz} beneath the gap lowers the value of $\Delta\sigma$ required for failure down to the base of the brittle layer, thereby weakening the entire crust beneath the gap. Slope-induced τ_{iz} levels increase with slope angle and are generally greater than the tectonically-

produced τ_{iz} beneath the slope inflections. Increased τ_{iz} reduces the magnitude of σ_3 relative to σ_{zz} , causing a shear stress weakening of the region. This shear stress effect is significant in the upper 5 to 10 kilometers of the crust, where the transition value (eq 3) may be locally exceeded, and decays with depth as a function of gap width, Poisson ratio (Savage and Swolfs, 1986), and of the lower crustal rheology.

The influence of topography upon the stress state in regions of extreme complex relief is demonstrated in figure 2 in which we present components of the stress tensor on a horizontal plane at 5 kilometers below sea level (13 km below Nanga Parbat summit) using the present topography in the NPHM region. The GTOPO30 data set used in production of figure 2A was re-sampled on a 50×50 grid (east-west spacing ~ 878 m; north-south spacing ~ 1110 m) with a vertical extent of 5 kilometers below sea level (fig. 2B). Stresses are calculated in the absence of tectonic forces for an elastic/Mohr Coulomb rheology with bulk modulus $= 10^{10}$ Pa, shear modulus $= 0.3 \times 10^{10}$ Pa, and $\phi = 35^\circ$ ($N = 3.69$) using the modified Lagrangian model described below. Effects of thermal weakening and cohesion are not considered at this point. At the level of topographic smoothing imposed by the sampling and grid density, very steep slopes encountered in NPHM (Bishop and Shroder, 2000) are not represented in the numerical grid. In addition, we have allowed plastic relaxation of the numerical topography to the angle of repose (35°) similar to the long wavelength average slopes suggested by Burbank and others (1996). Consequently, none of the grid is at failure at the time that the stress components presented in figure 2 were calculated and our values represent a minimum slope effect.

At 5 kilometers below sea level the distribution of stresses clearly reflects the topographic influence. As expected, the vertical normal stress, σ_{zz} , is increased beneath Nanga Parbat and other high elevations and reduced beneath the river valleys (fig. 2C). These perturbations are presented as the difference between those values derived from the natural topography and those assuming a constant elevation of 2 kilometers above sea level (fig. 2C). Consequently, positive values indicate areas of load strengthening and negative values reflect weakening due to the removal of load.

The extreme slopes of Nanga Parbat and the Indus valley walls to the north of Nanga Parbat concentrate vertical component shear stresses ($(\tau_{xz}^2 + \tau_{yz}^2)^{1/2}$) (fig. 2D) and bring these regions close to the point of failure throughout much of the upper crust.

The net influence upon stress distributions of the topography is to strengthen the regions beneath the high mountains and weaken the valleys. Weakening in the valleys results from both reduction in load and slope localization of shear stresses. Generally, these topographically-generated stress perturbations at 5 to 10 kilometers depth are on the order of 10 percent to 15 percent of σ_1 in compressional failure, but may approach 90 percent. We must emphasize that these are only general guides to stress perturbations and take no account of pore pressure fluctuations or spatial variation in density, cohesion, and friction angles.

In summary, shear stress weakening and reduction of vertical normal stress in valleys is sufficient to bring the entire crust close to failure adjacent to the valleys. Reduction in integrated crustal strength of ~ 15 percent in the proximity of either a forethrust or a backthrust results in concentration of deformation into that region, and a reduction in strain on the corresponding antithetic structure. Additional vertical advection of material into the gap, without erosion, reduces the gap relief and, consequently, the topographically-generated stress effect and its influence on strain patterns. Therefore, to maintain this weak region, the erosion mechanism within the valley must be capable of removing advected material and maintaining near steady state elevation within the valley.

Topographically induced stresses beneath mountains, however, lead to load strengthening, rigid translation of the massif, and are, by themselves, incompatible with the observed strain pattern within the massif (observations 6, 7 above). Geomorphic influence required to overcome this effect is discussed in the next section.

Influence of Exhumation

Because topographic effects by themselves can localize deformation but do not lead to actively straining isolated massifs, in this section we investigate the influence of exhumation upon lithospheric strength through its thermal effects. In a two layer continental crust with a brittle upper layer of thickness, h_{BD} , and a thermally activated ductile lower layer (Brace and Kohlstedt, 1980), the high strength brittle member provides most of the resistance to shear with a vertically integrated strength of

$$F_c \cong \int_0^{h_{BD}} \Delta\sigma dz = \frac{h_{BD}\Delta\sigma_{BD}}{2} \tag{4}$$

in which $\Delta\sigma_{BD}$ is the differential stress at the base of the brittle layer (Sonder and England, 1986).

The rapid decrease in shear resistance with temperature above $\sim 400^\circ\text{C}$ limits any contribution to the integrated strength of the lower crust to that region directly below the brittle-ductile transition (fig. 3). In the interest of producing working approximations, and because the shape of this transition is poorly known, with numerous rheological alternatives available (Evans and Kohlstedt, 1995), we approximate the strength contribution of the lower crust by the integral of the right triangle described by $\Delta\sigma_{BD}$ and the thickness of the transition zone, h_1 .

$$F_c \cong \int_0^{h_{BD}} \Delta\sigma dz + \int_{h_{BD}}^{h_1} \Delta\sigma dz = \frac{h_{BD}\Delta\sigma_{BD}}{2} + \frac{h_1\Delta\sigma_{BD}}{2} \tag{5}$$

For a brittle crust of 15 kilometers thickness, a transition zone of 3 kilometers into the temperature-dependent lower crust increases the crustal strength by ~ 20 percent. Because σ_3 does not differ greatly from σ_{zz} , $\Delta\sigma_{BD} \sim 2\sigma_{zz}$ and equation 5 can be recast as

$$F_c \cong (N - 1) \frac{\rho g h_{BD}^2}{2} + (N - 1) \frac{\rho g h_{BD} h_1}{2} \tag{6}$$

which, for a material with $\phi = 30^\circ$, reduces to

$$F_c \cong \rho g (h_{BD}^2 + h_{BD} h_1) \tag{7}$$

Equation 7 emphasizes the sensitivity of the integrated crustal strength to any variations in the thickness of the brittle layer.

THE EFFECTS OF TOPOGRAPHY ON REGIONAL STRAIN

Efficient erosion within a transverse valley is capable of maintaining a channel of approximately constant elevation despite vertical rock advection (Burbank and others, 1996). Application of this constant elevation condition to the topographic gap maintains the topographic stress perturbation of the gap allowing continued strain concentration into the gap. Continually removing material from the gap differentially exhumes deeper material within the gap with significant mechanical consequences. Advection into the gap of mass at vertical velocities in excess of 2 mm a^{-1} rapidly heats the upper 10 kilometers of crust, thereby thinning the high-strength brittle layer

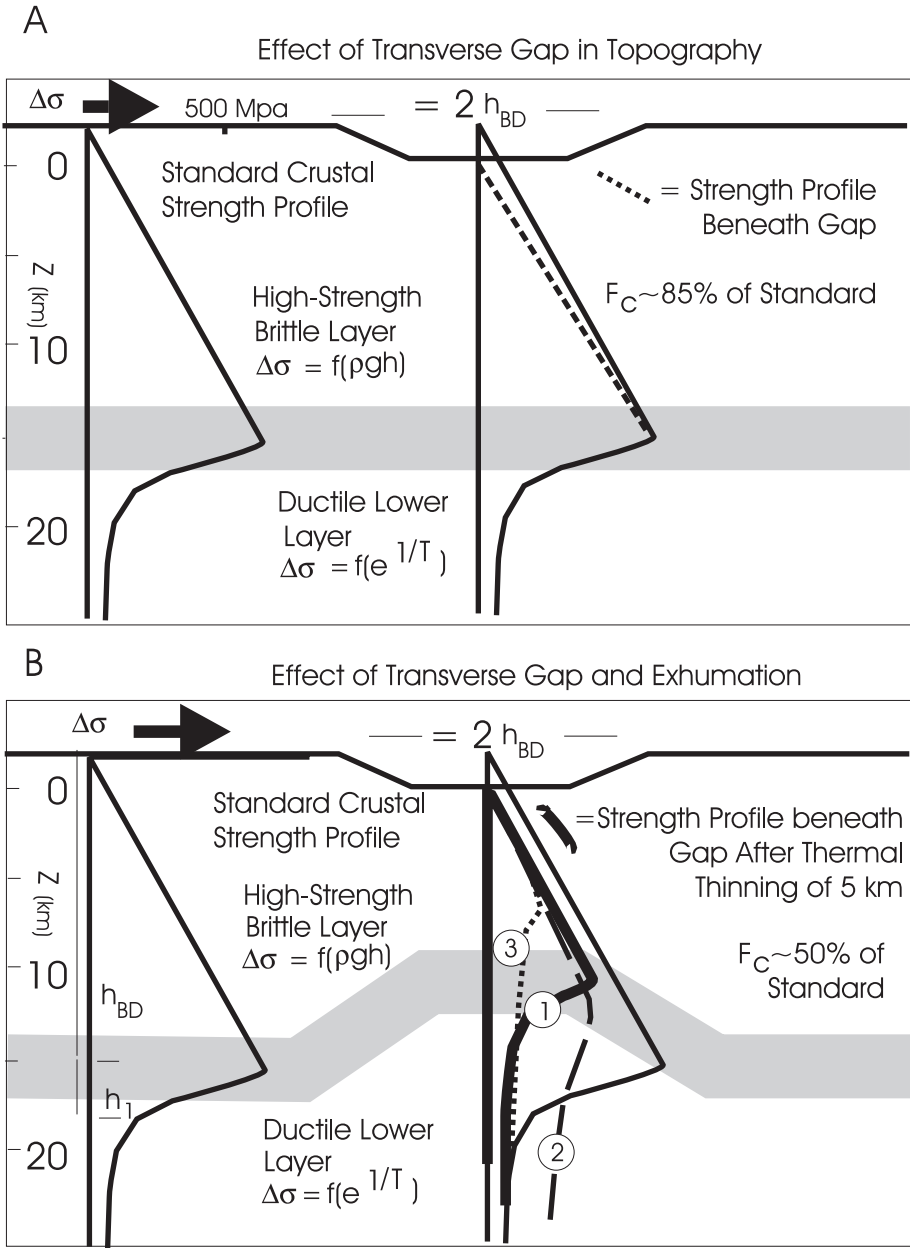


Fig. 3. (A) Crustal strength profile for a cohesionless quartz-dominated material of $\phi = 30^\circ$ for crust with no topographic relief, for the region beneath a transverse topographic gap. (B) Strength profile beneath the same gap after thermal thinning of the high-strength brittle region by 5 km due to differential exhumation. h_{BD} and h_1 used in equations 5, 6, 7 are shown in 3A. Curve 1 in 3B represents the calculated strength profile for a quartz-feldspar dominated crust (Ranalli, 1987) calculated from the analytical expressions in the text. Curve 2 is taken from the un-thinned model crust (fig. 6B). Curve 3 comes from the thermally thinned central massif of the numerical model (fig. 6B). The topographic gap modifies the upper portion of the crustal strength envelope, while thermal thinning removes the highest strength part of the continental crust.

(Koons, 1987; Craw and others, 1994). As mentioned previously, seismic observations (Sarker and others, 1999; Meltzer and others, 2001; Zeitler and others, 2001a) and fluid inclusion data of an elevated geothermal gradient of the NPHM (Craw and others, 1994; Winslow and others, 1995; Zeitler and others, 2001b) indicate shallowing of the ductile to brittle transition beneath Nanga Parbat to a depth of less than 10 kilometers beneath the surface.

The influence on crustal strength of thermal thinning differs somewhat from that due to a topographic gap described above in that rapid exhumation removes the lower, highest strength part of the brittle crust. Both the thickness, h , and the differential stress at the base of the brittle layer, $\Delta\sigma_{BD}$, which is also a function of h , are reduced by upward advection of isotherms. In the one-dimensional approximation used above, reduction of the thickness of the crust from 15 to 10 kilometers, reduces the contribution of the brittle layer to the total integrated strength by ~ 50 percent. This effect is reduced in three dimensions where shear resistance at the margins of the rheological anomaly contributes to the total shear resistance, however, rheological weak spots of approximately the same dimension as the thickness of the high-strength brittle region significantly reduce the integrated strength of the entire crust and further localize deformation within that weakened region. Although the absolute amount of weakening that accompanies exhumation is a function of the rheological behavior at the brittle/ductile transition, given the high thermal inertia of silicates, the general effect depends upon vertical advection of lower crust with a shear resistance inversely related to temperature.

The combined mechanical effect of a topographic gap, adjacent to either forethrust or backthrust, and channel erosion sufficiently efficient to maintain a channel at near-constant elevation produces a mechanical weak spot that becomes weaker with exhumation. The initial cutting of a topographic gap with no exhumation decreases the crustal strength by an amount dependent upon the total relief and the width of the gap. In some instances such as the region adjacent to the Indus valley (fig. 2D) topographic relief is sufficient to bring much of the upper crust to failure. Less dramatic relief can readily reduce the integrated strength by ~ 15 percent. Strain concentration within this gap accelerates as thermal thinning further reduces the thickness of the brittle layer, reducing the total integrated strength in the zone of exhumation by greater than 50 percent of the original strength. The rheological contribution to crustal strength dominates after approximately 5 kilometers of differential exhumation and the influence of topographic load diminishes in importance. The metamorphic and thermal effects of this geomorphically induced aneurysm are discussed below and also contribute to a reduction in local crustal strength.

NPHM MODEL

To investigate the metamorphic implications of exhumation in the NPHM, we employ a model geometry of 50 kilometers thick by 500 kilometers square with a cell density that increases toward the center at x (north) = y (east) = 250 km (fig. 4). In our numerical models, two continents with layered rheology are collided along an originally east-west plate boundary (fig. 4) roughly simulating collision of India and Eurasia. The end and base of the model Indian block move northward into model Eurasia at a velocity ($=V_x$) fixed along the base. Lateral boundaries of the model are sufficiently distant from deformation that they do not influence the solution (figs. 4 and 5). An elevation step of 4 kilometers simulating the Tibetan Plateau is added to the northern half of the model.

In the standard initial models, a pressure-dependent Mohr-Coulomb rheology ($\phi = 35^\circ$) is employed for the upper 15 kilometers of crust underlain by pressure-independent elastic-plastic material increasing in thickness to 35 kilometers from south to north above the northward dipping base. Plasticity follows a von Mises model

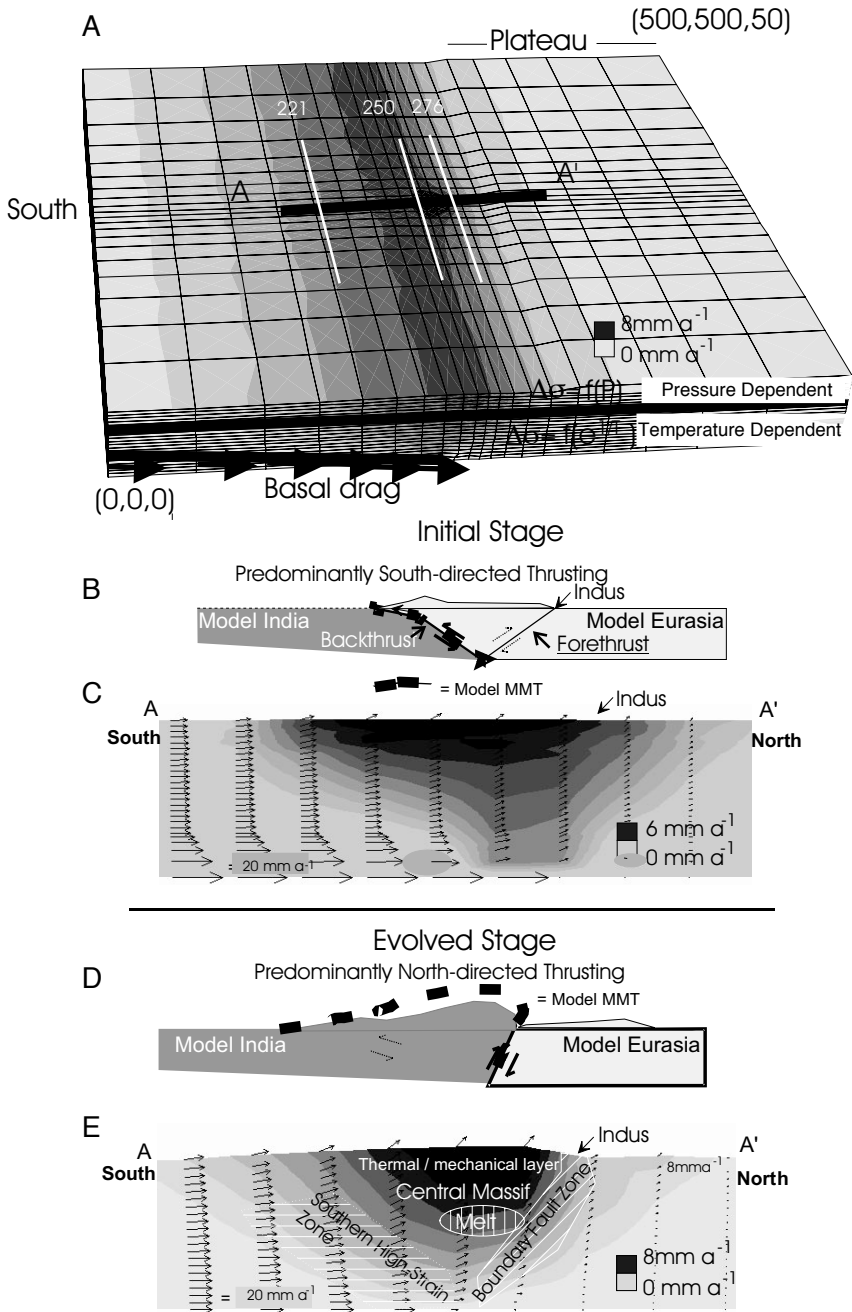


Fig. 4. (A) Oblique view of NPHM mechanical model with contoured vertical velocity (dark fill = highest rates). The velocity distribution on the exposed eastern vertical section is the pattern produced in the absence of the lateral rheological differences associated with thermal thinning. The dome in the vertical velocity is associated with rapid exhumation in the region of the incising river and advection hotspot. A-A' identify the north-south sections in subsequent figures and the numbers 221, 250, 276 identify the positions of East-West cross-sections presented in subsequent figures. (B) Initial Stage: Schematic geological interpretation along A-A' cross-section. South-directed thrusting dominates at this early stage. MMT serves as a marker horizon separating India from Kohistan/Eurasia. (C) North-south view of vertical velocity along section A-A' adjacent to the incising river. Vectors identify total velocity along this cross-section. (D) Evolved Stage: Schematic interpretation showing dominantly north-directed thrusting of hot, deep model Indian material through the overlying plate. Predominantly north-dipping reverse structures extend to the south of the model massif where strain is distributed over a wider area than to the north (compare with Kidd and others, 1998; Schneider and others, 1999b). (E) Vertical velocity along A-A' section after advection of deeper weak rocks adjacent to the incising river.

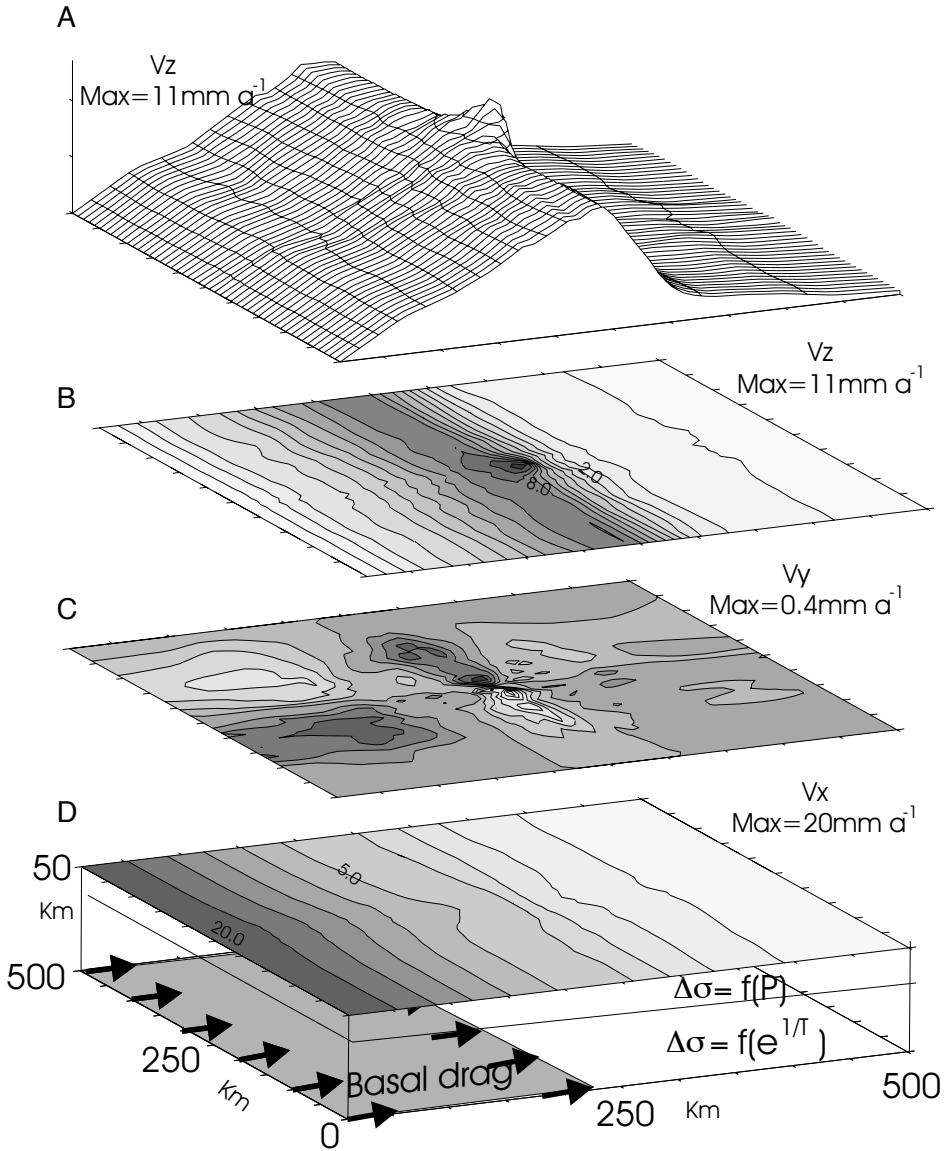


Fig. 5. Contours of horizontal and vertical velocity components in the NPHM model of figure 4A. Concentration of deformation into the thermally weakened position is obvious for all components, but is most important for the vertical component as illustrated in the surface diagram.

(Terzaghi, 1943) and is inversely related to temperature (for example Brace and Kohlstedt, 1980) mimicking the empirically derived plagioclase-dominated strength profile (fig. 2) (Ranalli, 1987). Stress rates in post-yield flow are governed by a non-associated flow law that is a function of local strain rates. Solution of the mechanical equations in three dimensions is accomplished via a velocity based, Lagrangian formulation (ITASCA; Cundall and Board, 1988) modified to accommodate large strains and localized erosion. The method and software are similar to that employed previously for geotechnical and geodynamic analysis (for example Hobbs

and others, 1990; Upton and others, 1995; Ord and Oliver, 1997; Upton, 1998; Koons and others, 1998) and use an explicit finite-difference solution for elastic and plastic materials. The equations of motion are solved at the grid nodes for spatial and velocity derivatives discretized between nodes over constant strain rate tetrahedral elements. All results are presented within an externally fixed reference frame.

In this phase of the mechanical modeling, we concentrate on the metamorphic evolution of a region adjacent to an incising river (fig. 4) with emphasis on the evolved stage. The rheological profile where exhumation is greatest is calculated from the solution of the two-dimensional transient heatflow equation for an advecting medium in the presence of topography

$$\frac{\partial T}{\partial t} = \kappa \left(\frac{\partial^2 T}{\partial x^2} + \frac{\partial^2 T}{\partial z^2} \right) + V_z \frac{\partial T}{\partial z} + V_x \frac{\partial T}{\partial x} \quad (8)$$

(Koons, 1987; Craw and others, 1994; Batt and Braun, 1997). We have chosen an intermediate value for thermal diffusivity ($\kappa = 10^{-6} \text{ m}^2 \text{ s}^{-1}$). The velocity vectors for the last terms on the right of equation 8 are taken from the mechanical solution. Consequently, the thermal and mechanical responses are coupled through the rheological dependence upon temperature. Strength profiles for the initial and thermally weakened regions within the numerical models are presented in figures 2 and 6.

We model the role of erosion by assuming, following Burbank and others (1996), that large rivers, specifically the Indus, are capable of maintaining effectively constant grade throughout orogenesis. Based upon this assumption, we have fixed the elevation along the model valley, removing all material that passes through that steady state elevation. Ridges and mountains develop freely around the valley, with slopes controlled by the internal angle of friction of the material. This scheme produces an effectively constant elevation valley with growing mountains of approximately constant slopes similar to the large scale average of 35° measured by Burbank and others (1996) with slope transport dominated by landsliding. The higher angle slopes recorded by higher resolution terrain analysis (Bishop and Shroder, 2000) require material cohesion that we have not included in this study.

RESULTS

Collision in the initial, laterally homogeneous model produces a near-symmetrical block mountain range situated above the leading edge of subducting mantle and bounded by forethrust and backthrust. These features are identical to 2-dimensional simulations described elsewhere (for example Willet and others, 1993; Beaumont and others, 1996). The width of the mountain range is a function of the thickness of the deforming block and the relative strengths of the upper and lower crusts with a relatively weaker lower crust producing a wider zone of deformation (Davis and others, 1983; Davis and Lillie, 1993; Ellis, 1996).

The position of a deformation front in a simple convergent orogen, without variation in the boundary velocities, is controlled by the relative magnitudes of shear resistance along three regions: the orogen base, the forethrust and the backthrust (fig. 4). Shifting of the main deformation front at the surface reflects a shift in the relative balance of these three elements.

With the imposition of a topographic plateau to the north simulating the Kohistan block, the initial wedge-type of deformation is dominantly south-directed on north-dipping structures (fig. 4) due to topographic localization of strain south of a pre-existing plateau (England and Searle, 1986). Enhanced exhumation along the river channel leads to thermal thinning of the strong brittle layer within a zone that dips steeply to the south. The results are given in schematic form in figure 4, while trajectories, velocities, stress levels and strain rates for the evolved aneurysm are

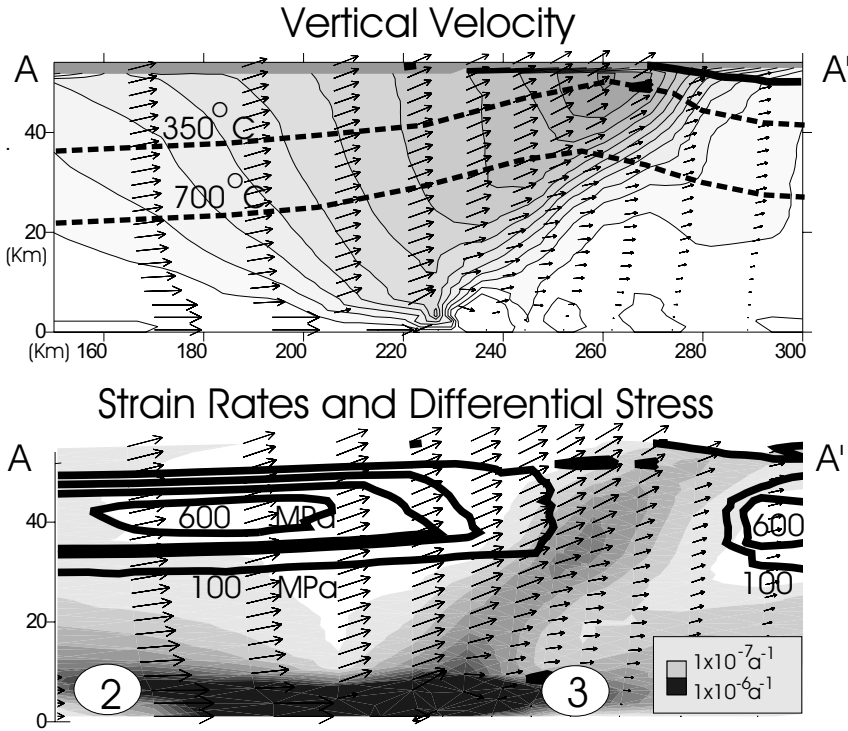


Fig. 6. (A) Cross-section through the massif along A-A' showing contours of the vertical velocity, local particle trajectories and position of the 350°C and 700°C isotherms calculated through equation 8. (B) Contours of the differential stress (heavy lines; MPa) superimposed upon shear strain rate field (dark fill = highest rates) for section A-A'. The massifs is identifiable as a high strain, low stress anomaly. Numbers 2 and 3 identify the location of the vertical differential stress profiles plotted in figure 3.

provided in a more detailed form in subsequent figures. Thermal thinning due to exhumation along a channel of less than 5 kilometers depth readily produces a rheological weak spot within the crust as indicated by the region of low differential stress within the Central Massif. The presence of the weak spot influences the choice of dominant thrusting direction within the orogen. Weakening within an initially symmetric orogen leads to spots of dominantly north-directed shortening associated with the weak spot where lower plate material pokes up into and displaces the upper plate (figs. 4 and 5).

Once deformation becomes concentrated along the thermally weakened zone, the velocity pattern of figures 5 and 6 becomes increasingly stable due to positive feedback of advection and deformation. The three-dimensional nature of this hot spot is clear within the east-west cross-sectional views of vertical velocity and shear strain rates (fig. 7). This evolved velocity field has four characteristic features, to which we make frequent reference (fig. 4). These are:

- The Boundary Fault: South dipping; effective northern limit of deformation;
- Southern High-Strain Zone: North-dipping high-strain zone south of massif;
- Central Massif of rapid exhumation beneath the summit, and
- Thermal/mechanical boundary layer of steep mechanical and thermal gradients in the upper crust.

Material moves from the south into the Central Massif with strain initially distributed to north and south of the uplifting wedge. Material moving in from the

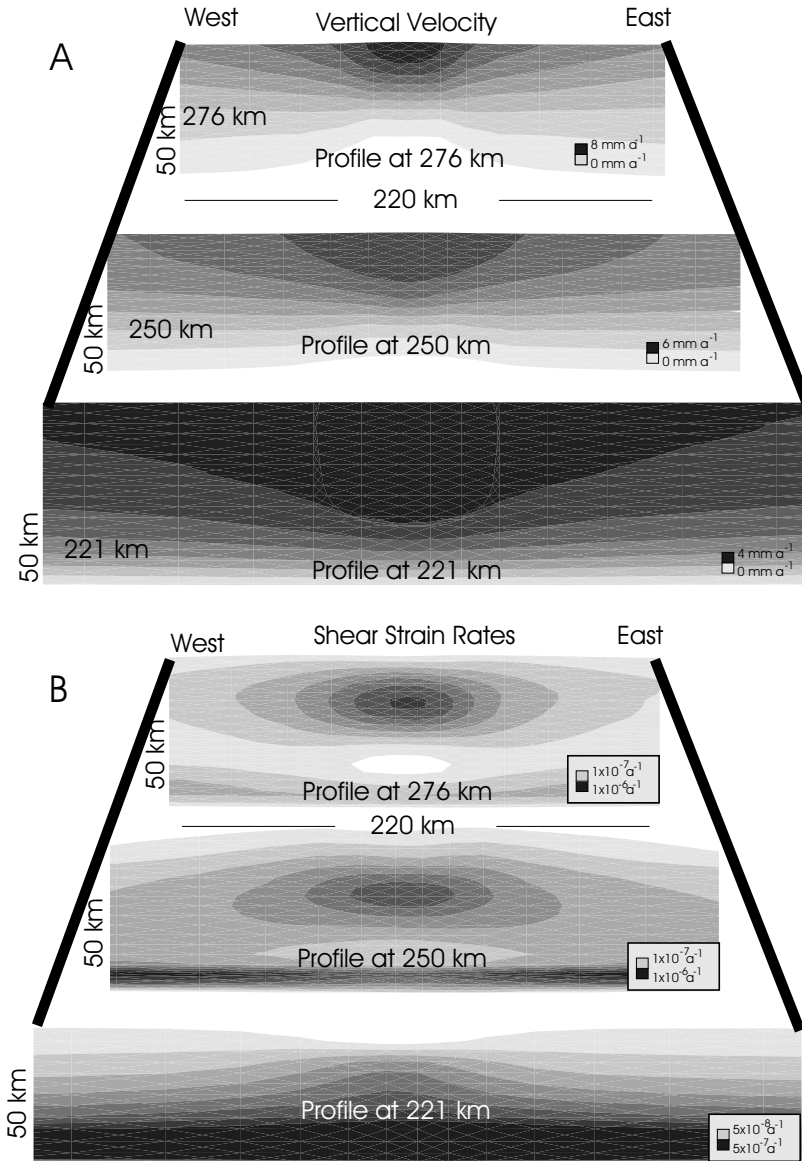


Fig. 7. Shear strain rate and vertical velocity field (dark fill = highest rates) within east-west planes to the south of the massif (221) through the massif (250) and at the northern edge of the aneurysm (276). The numbers refer to the distance in kilometers from the southern edge of the NPHM model along profiles identified in figure 4.

south decelerates to ~ 0.5 convergence rate as it passes through the Southern High-Strain Zone (high-strain zone to the south of the massif). Where the river-erosion condition exists, material is preferentially concentrated to the northern side of the orogen (figs. 5 and 6) leading to advection of deeper, weaker material into the region immediately south of the model river. In the early stages of convergence prior to thermal weakening, most of the remaining strain is accommodated along this south-dipping structure that forms the northern boundary of the evolving metamorphic

massif. It is along this high-strain zone that most material exits the massif. Initially, topographic growth occurs over a broad region as block uplift (Beaumont and others, 1992) with the erosional gap forming an increasingly deep topographic gap. Evidence for such broad block uplift can be seen in a regional younging of fission-track ages towards the NPHM (Zeitler, 1985).

Advection of lower-crustal material into the eroding zone heats, weakens and further concentrates uplift in the region causing lower-crustal material to flow into the deforming region from all sides. As deformation continues, the thermal weakening under the uplifting model massif becomes sufficient to shift the location of greatest vertical velocity southward toward the weakened mass, even though the vertical load is greater under this mass than beneath the adjacent model river gorge. That is, the rheological weakening becomes a greater influence than the load strengthening. Vertical velocity in the massif region is equivalent to the local horizontal velocity. The rate of topographic growth of the massif depends upon local erosion rates and will approach the vertical velocity in arid regions. One topographic result of this strain concentration is the formation of very high isolated massifs.

Within the upper 5 to 10 kilometers of the modeled massif, the aneurysm velocity pattern (fig. 6) produces topography, compresses isotherms and compacts the zone of transition from predominantly ductile deformation to predominantly brittle failure (Koons, 1987; Meltzer and others, 2001). The steep gradients of topography, temperature and strain rate within this thermal/mechanical boundary layer are potent driving forces for fluid flow and provide an explanation for active hydrothermal systems such as those seen along the Nanga Parbat massif margins as discussed in the companion paper (Chamberlain and others, 2002). After ~ 1 Ma of exhumation, a near-steady state thermal pattern is established through which rock passes as the massif is exhumed. Near surface geothermal gradients of $\sim 60^\circ\text{C}/\text{km}$ are produced and the 400°C isotherm is elevated to ~ 8 kilometers below the surface, consistent with observations made at Nanga Parbat (Winslow and others, 1995; Craw and others, 1997). Although local perturbations resulting from fluid advection patterns may occur, the general thermal pattern remains stable for similar exhumation conditions and the hydrothermal system centered about the mountain serves as a very efficient cooling tower identified by the distribution of microseismicity (Meltzer and others, 1996, 2001).

In summary, the topographic gap in the Kohistan block of 25 to 50 kilometers and the continued erosion within this gap by the Indus produce a rheological weak spot that focuses deformation into a relatively small region due to the positive feedback of thermal weakening and strain. This positive feedback permits the growth of extreme elevations in a large, internally deforming massif. Without the positive feedback, deformation would be deflected away from a massif. The Central Massif, with its Southern High-Strain Zone, central hot spot, and cooling tower is fixed within the crust and is visible within a geophysical reference frame by its electromagnetic and seismic signatures (Park and Mackie, 1997, 2000; Meltzer and others, 2001).

SENSITIVITY AND LIMITS OF THE NUMERICAL MODEL

The concentration of deformation accompanying exhumation is a function of the crustal rheological model that in detail is poorly constrained (Evans and Kohlstedt, 1995). The amplitude and timing of the aneurysm are sensitive to this rheological model. The general response depends not on the details of the model, however, but upon the assumption that the flow resistance in a quartz- or feldspar-dominated crust is inversely related to temperature for $T > \sim 350^\circ\text{C}$. If the lower crust is not weaker than the upper (for example Maggi and others, 2000), then exhumation will not produce the thermal weakening effect invoked here. The seismological evidence of an upwardly bowed lower limit to seismicity and low seismic velocities (Sarker and others,

1999; Meltzer and others, 2001; Zeitler and others, 2001a) indicates that at Nanga Parbat, at least, the exhumation of deep crust is associated with reduced elastic moduli.

With the emphasis in this paper on the relationship of metamorphism to exhumation, we have assumed a steady state elevation of river valleys and not explored the evolution of a fully coupled surface model with the mechanical evolution. We have examined in detail the trajectories associated with the present state of the massif, but have not followed the full geomorphic and geological evolution of the massif over the past 10 Ma. Particle trajectories are sensitive to the spatial pattern of erosion, but the first order control on the degree of coupling between exhumation and rheology is exerted through maintenance at constant elevation of a region of approximately the thickness of the brittle layer during deformation. The gap in the Kohistan block of between 25 and 50 kilometers meets the topographic constraints and the Indus, with its tributaries of the Astor, Gilgit and Hunza rivers, has apparently maintained a roughly constant grade for millions of years (Burbank and others, 1996; Zeitler and others, 2001b). Integration of a surface process model utilizing further knowledge of erosion rates as a function of altitude and climatic variation in the western Himalaya (Shroder and Bishop, 2000), with the mechanical model could provide more detailed information on massif evolution.

The thermally dependent rheological parameters of the three-dimensional model rely upon a two-dimensional thermal solution to the nonlinear advection equations. Given the high relief on the topographic surface, the presence of active thermal and topographic convection within the upper crust, the two-dimensional approximation appears appropriate. In addition to the particle velocity field, the thermal solution is sensitive to the choice of temperature structure with depth, thermal diffusivity of the advecting rock, the near surface permeability structure, and the detailed topographic shape of the massif (Koons, 1987). With uncertainties in all of these parameters, the error introduced by approximation of the three-dimensional thermal state with a two-dimensional solution is not great. In addition, we have used observations pertinent to the thermal state to constrain the lateral limit of the NPHM thermal anomaly (Zeitler and others, 2001a).

Because we are aware of no reliable constraints upon the amount of material partitioned into crustal root growth, we have assumed that material entering the deforming zone does not subduct or become shunted outside of the deforming model. Consequently, there is no contribution to crustal root growth due to crustal underplating and the models provide no information on this component of collision. In the following section we partition half of the available relative plate velocity into this deforming zone and assume that the remainder is distributed throughout the orogen.

We have assumed that an initial topography existed to the north of the deforming zone similar to the Kohistan block. Although suggested by geochronological information, reconstruction of western syntaxis topography over the past 10 Ma is problematic. The numerical results are not sensitive to the magnitude of this plateau.

IMPLICATIONS FOR METAMORPHIC EVOLUTION: MINERALOGICAL STABILITY REGIONS WITHIN THE CENTRAL MASSIF

By combining the numerically derived velocity pattern with simple two-dimensional thermal modeling of rapidly exhuming terranes (Craw and others, 1994) it is possible to identify pressure and temperature (P-T) regions of predicted mineralogical stability and fix these P-T coordinates within the geophysical reference frame of the Central Massif. We have mapped onto the spatial dimensions of figure 8A the equilibrium stability regions of several reference assemblages from the deep crust including the aluminosilicate system and dry melt.

In the undisturbed state, most of the crust resides within kyanite stability depending upon the curvature of the geotherm at depth (England and Thompson, 1984). As

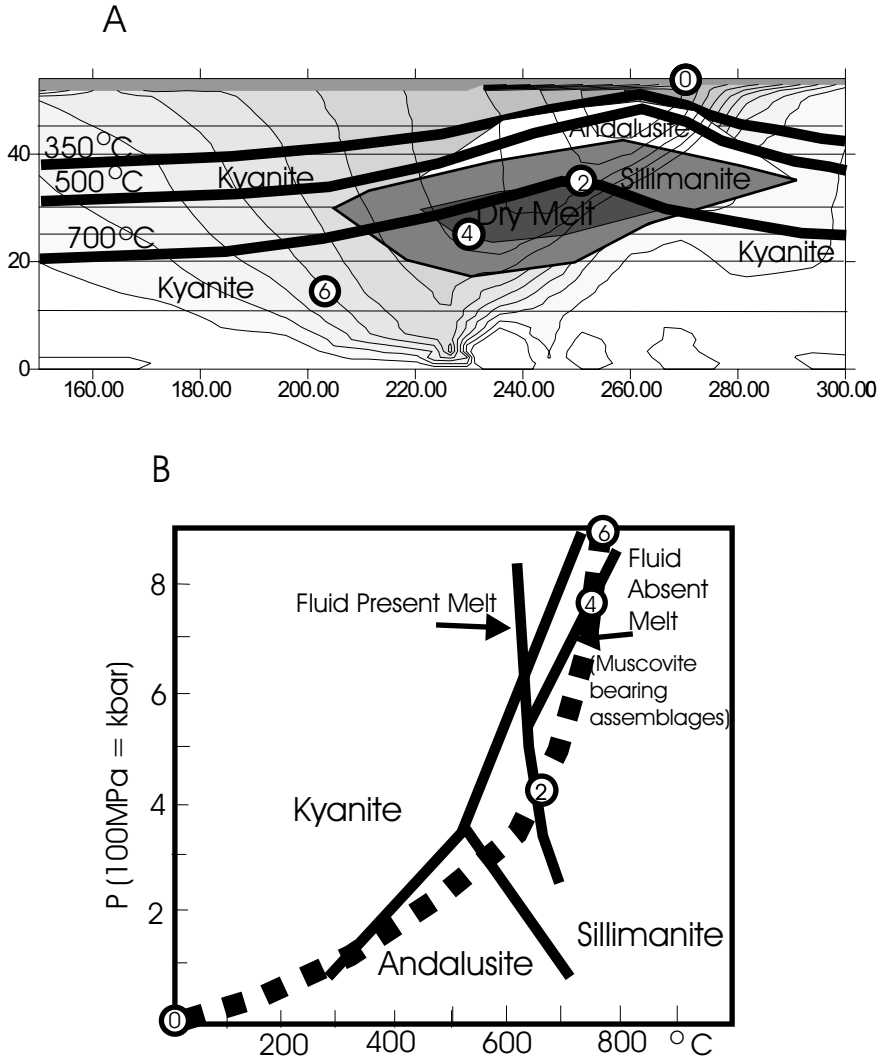


Fig. 8. (A) P T stabilities of aluminosilicates, and minimum melts superimposed upon the evolved velocity structure of figure 5. Positions of the rock/fluid packet tracked through the massif are indicated as time before present in Ma. (B) PT diagram showing positions of the same packet tracked for 6 Ma in 8A relative to equilibrium boundaries and geothermal gradients. Dotted curved trajectory indicates the geotherm for the evolved velocity model of figure 8A. Muscovite melting relationship from Pattino-Douce and Harris (1998).

originally predicted by Albarede (1976) from a one-dimensional thermal analysis, the pattern of petrological stability changes significantly with concentrated advection of deep crustal material. In two and three dimensions concentrated advection produces a lozenge-shaped region of sillimanite stability at ~ 20 kilometers below the surface (fig. 8A, B). With further advection, the lozenge expands and within it another lozenge of dry melt stability for muscovite-bearing assemblages (Pattino-Douce and Harris, 1998) is exceeded. Above the sillimanite lozenge, andalusite becomes stable within the upper 10 kilometers of the advection hotspot while the stability of kyanite shifts to the edges of the massif and below the sillimanite lozenge. Given the initial geotherm, this pattern

forms after ~ 1 Ma and remains stable for as long as material is exhumed within this massif.

ASSEMBLAGE EVOLUTION

The spatial distribution of mineral stability regions remains relatively fixed in the crust even though rocks are continuously moving through the massif during deformation and exhumation. Rocks may have distinct P-T histories, which depend, in part, upon where they enter and exit the orogen (Jamieson and Beaumont, 1988). As an example, we track the most recent 6 Ma history of a rock/fluid packet of pelitic composition, initially residing at ~ 35 kilometers within the kyanite stability field and presently exposed at the surface. Assuming that about half of a typical Himalayan plate convergence rate of 40 mm a^{-1} can be accommodated locally (De Mets and others, 1990), with the remainder distributed across the collision zone and into a poorly constrained crustal root, a rock packet from ~ 35 kilometers depth resides in the 25 to 40 kilometers wide north-dipping Southern High-Strain Zone for about 2.0 Ma (6 on fig. 8A, B). The precise transit time within the straining region depends upon the degree of strain localization and could be as low as 0.5 Ma.

Transit through the Southern High-Strain Zone does not subject the rock to either steep thermal or pressure gradients. Nonetheless, metamorphic equilibration and volatile release can occur as the rock enters this high-strain zone (Koons and others, 1998; Zeitler and others, 2001a). Fluids generated in such a region and rising through the deforming mass appear as fluid inclusions within overlying, overthrusting gneisses (Winslow and others, 1995; Craw and others, 1997), and may, for example, be the source of high electrical conductivity seen to the south of Nanga Parbat (Park and Mackie, 2000; Chamberlain and others, 2002).

The temperature of the rock/fluid packet remains constant as it passes beyond the Southern High-Strain Zone while it decompresses at $\sim 1.5 \text{ kbar Ma}^{-1}$. The rock packet then passes into the growing sillimanite and dry melt lozenges where the rapid decompression of water-poor, dehydrated gneisses generates vapor-absent granitic melts which are emplaced upwards into the model massif (4 on fig. 8A, B). Rock dehydrated by passage through the Southern High-Strain Zone then passes into a lower-strain zone beneath the summit, with the advection of isotherms elevating the position of the brittle/ductile transition. Isotherms diverge most from an unperturbed state in the 20 to 10 kilometers below the surface where material continues to decompress nearly isothermally at 1.5 kbar Ma^{-1} . The greatest vertical velocities, attained immediately north of the summit, are 6 to 8 mm a^{-1} and material can be exhumed from 20 kilometers depth within ~ 3 Ma.

The rapid exhumation of rocks just north of the summit results in: 1) rapid decompression P-T paths; 2) concentric isograd/isobar patterns which expose granulite facies, low pressure rocks in the core of the massif, bordered by higher pressure and lower-grade amphibolite zone rocks on the edges of the massif; 3) a concentric pattern of young cooling ages in the high-grade core of the massif; and 4) an active hydrothermal fluid system where isotopic systems are increasingly influenced by high altitude meteoric fluids (Chamberlain and others, 1995, 2002).

As thermal weakening proceeds, vertical motion is shifted south from the model river where elevations are fixed by erosion into the region of greatest total uplift. Thermally-induced rheological weakening reduces the relative influence of erosion in concentrating strain to the point that strain becomes localized into the highest and weakest peak. With the relative plate rates quoted above, the model horizontal velocity at the surface to the north of the massif is $\sim 8 \text{ mm a}^{-1}$.

APPLICATION OF MECHANICAL/EROSIONAL COUPLING TO THE EASTERN SYNTAXIS

Although the relative plate vectors on the Himalayan Eastern Syntaxis differs from that in NPHM, with large lateral velocity gradients, the Eastern Syntaxis does exhibit extreme topography and apparently young metamorphism similar to the NPHM. (Burg and others, 1997; Koons and Zeitler, 1997). Those mechanical elements present in NPHM related to rheological evolution through erosional/ mechanical coupling also appear to be present near Namche Barwa; that is efficient incision by the Tsangpo in the vicinity of a predicted forethrust and an advection-related thermal anomaly (Hochstein and Yang, 1992). On this basis, we have produced two mechanical models of the eastern syntaxis; one that does not incorporate erosional/rheological coupling and one similar to the above model of NPHM in which advection and concentrated exhumation leads to thermal thinning (fig. 9). The boundary conditions of these models differ from those of the above mature NPHM model only in the imposition of an eastern limit in the northwards plate velocity at $y = 200$ kilometers and do not consider the additional effect of the Tibetan plateau.

Introduction of the model velocity corner in the east produces a clockwise rotation of the velocity field in the corner region (fig. 9A) (England and Houseman, 1986; Royden and others, 1997; Shen and others, 2001) with strain accommodated by a series of reverse faults and along steep strike-slip structures. This velocity pattern is similar to that determined from moment tensor analysis (Holt and others, 1995; Hallet and Molnar, 2001), analysis of mantle anisotropy (Holt, 2000), and is broadly consistent with surficial geological mapping (Burg and others, 1997). In the first model in which no weakening is permitted, exhumation is significantly less than in NPMH, and occurs well to the west of the velocity corner.

The model conditions reproduce observations of spatial concentration of rotation (for example Holt and others, 1995; Holt 2000), but they do not produce the concentrated exhumation suggested by metamorphic analysis of the region. The application of the same rheological model applied in the NPHM model associated with a model Tsangpo at the eastern orogen edge concentrates shortening adjacent to the corner (fig. 9B). The consequence of this weakening is not obvious in the velocity maps of either horizontal component, but is clearly seen in concentration of exhumation at the corner. This model predicts, therefore, that many of the distinctive PTt paths, seismicity patterns and geomorphic features observed in the Nanga Parbat region are also present in the eastern syntaxis where the Tsangpo is actively incising the very deep gorge. In addition, intense exhumation along the river gorge is partly responsible for the low contractional signal in geodetic measurements along the eastern plateau edge (King and others, 1997).

CONCLUSIONS

Local erosional and rheological variation can produce significant changes in the shape of an orogen despite constant far field velocities. Generally, a simple topographic load strengthens the crust, deflecting strain around the load. Consequently, deflection of deformation into regions of extreme topography rather than away from the load indicates significant reduction of crustal strength relative to the unperturbed state. A requirement of the aneurysm behavior is that the mechanism that produces the topographic load also weakens the crust so that strain is partitioned into the load rather than around it. One means of coupling the production of the load to localized weakening of the crust is through the thermal influence of sustained exhumation on crustal rheology. Transverse rivers capable of maintaining an approximately steady-state gradient through advecting material can initiate steep regions of rheological weakness within a collisional orogen.

Requirements for geomorphic influence at a fluvial scale are:

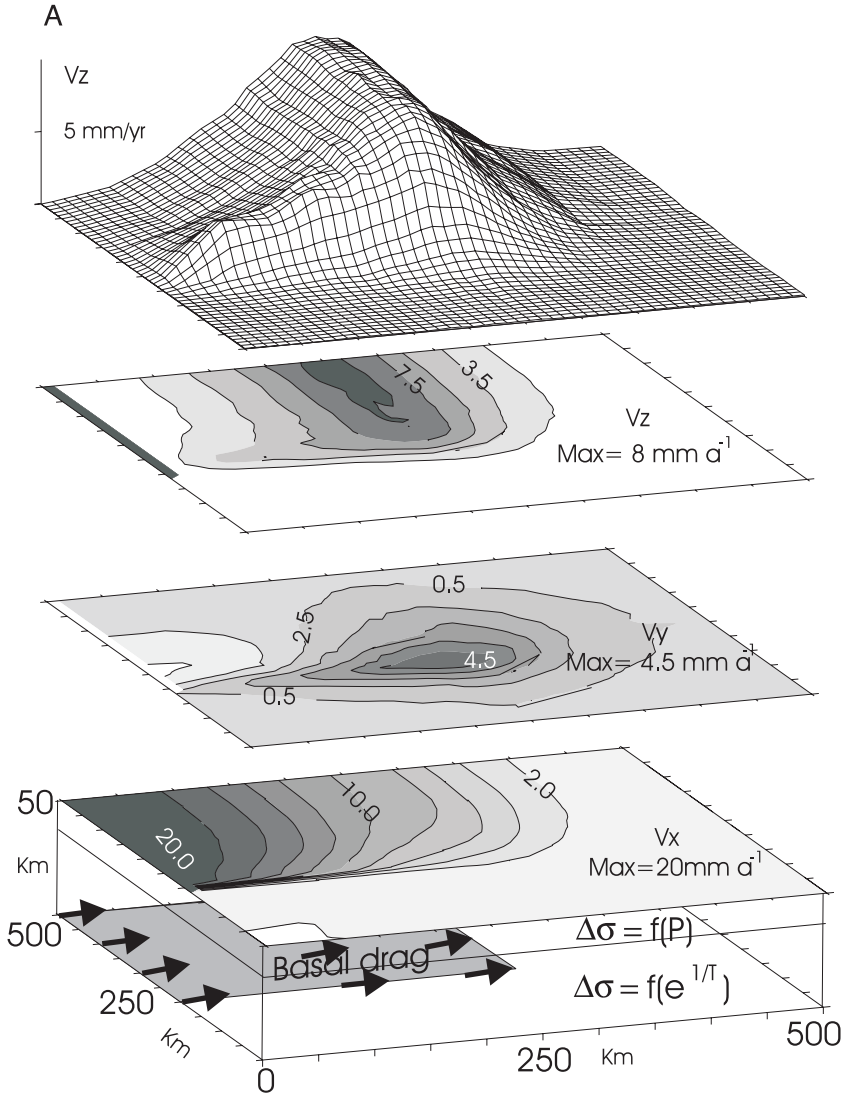


Fig. 9. Regional mechanical model similar to the NPHM model displayed in figure 5, for the Eastern Syntaxis adjacent to the Tsangpo gorge. (A) Velocities for model with no thermal thinning.

I. Crust must have a layered rheology with the upper layer capable of supporting greater shear stresses than the lower crust.

II. In order to have a significant influence on collisional strain patterns, a transverse topographic gap must be of a width at least as great as the thickness of the upper, high strength brittle layer.

III. Fluvial erosion must be sufficient to maintain the approximate dimension and position of the topographic gap.

IV. The gap must be initiated near either forethrust or backthrust where the region is already close to failure.

These conditions are met by the Indus (Burbank and others, 1996) and, apparently, the Tsangpo on the eastern Himalayan syntaxis.

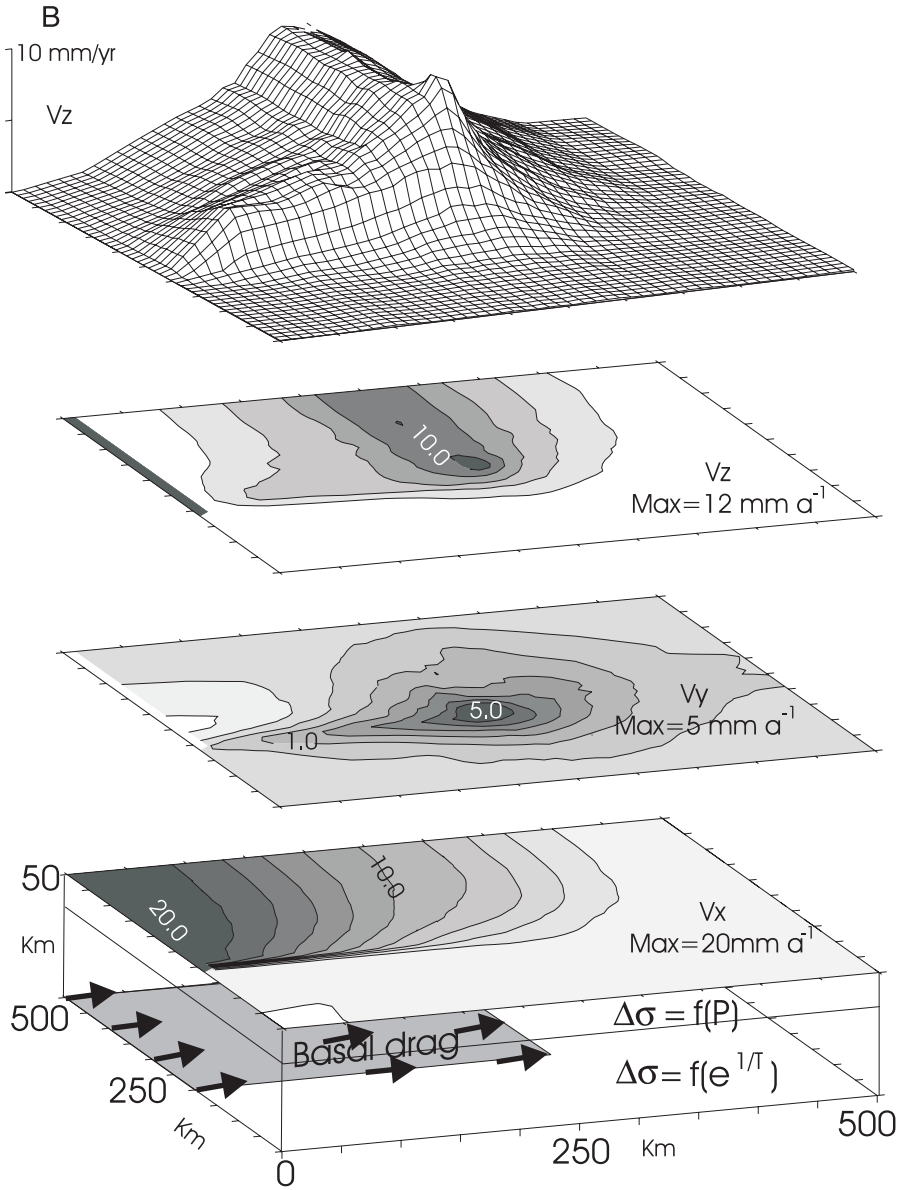


Fig. 9. (B) Model velocities generated with erosional/mechanical conditions used in NPHM that incorporate thermal thinning associated with the Tsangpo gorge. The effect of thermal thinning related to exhumation is to further concentrate exhumation at the eastern corner.

The petrological and geophysical signatures of this geomorphic influence are dramatic. River-induced thermal thinning produces crustal antiform structures directed in an opposite sense to the remainder of the orogen as in Nanga Parbat (Coward and Butler, 1985) and Namche Barwa (Burg and others, 1997). Erosion becomes increasingly less important as a control on the velocity pattern as thermal thinning proceeds and rheological weakening assumes a dominant role.

Positive feedback of thermal weakening and strain concentration within the vertical weak zones results in the formation of a stable hot spot that serves as a crustal foundry for production and exhumation of high-temperature assemblages. Discrete stability lozenges first of high-temperature assemblages, then of crustal melt, grow within a Central Massif. Growth of the melt lozenge further increases the feedback mechanisms of deformation and weakening capable of producing a tectonic surge (Hollister and Crawford, 1986; Butler and others, 1997). Metamorphic equilibration occurs as rocks pass through these lozenges at a rate of $\sim 5 \text{ km Ma}^{-1}$. Steep gradients in the driving forces for fluid flow produce active hydrothermal systems as rock passes into the thermal/mechanical boundary layer of rapid cooling (Craw and others, 1994; Chamberlain and others, 2002).

The petrological result of strain concentration within this tectonic aneurysm is one of a domal pattern of young, high temperature gneisses surrounded by lower temperature, higher pressure assemblages with steep PT field gradients. The feedback process is one of concentration, therefore the geological pattern should be one of increased metamorphic grade at reduced spatial scales. We suggest that at least some of the ancient domal outcrop patterns of high-temperature assemblages such as the “pop-up” structures of the Central Maine Terrane in the Appalachians (Chamberlain and Lyons, 1983) represent velocity focusing due to rheological weakening and may reflect the scale of surficial processes at the time of formation. Whether the specific trigger for concentration is erosional or rheological, coupling between the two can explain the presence of topographically high-standing, active metamorphic massifs like Nanga Parbat and Namche Barwa at the ends of the Himalayan chain (Burg and others, 1997; Koons and Zeitler, 1997).

ACKNOWLEDGMENTS

Throughout the Nanga Parbat Continental Dynamics Project, we have been fortunate to have shared comments, criticism, and ideas with Leonardo Seeber, Bill Kidd, Mike Edwards, Dave Schneider, Jack Shroder, Mike Bishop, Valerie Sloan, Phaedra Upton, Terry Pavlis and others. Presentation has been greatly aided by the critical reviews of T. Pavlis, J. Platt and an anonymous reviewer. This project was supported by the U.S. National Science Foundation’s Continental Dynamics Program.

REFERENCES

- Albarede, F., 1976, Thermal models of post-tectonic decompression as exemplified by the Haut Allier granulites (Massif Central, France): *Bulletin Société Géologie France*, v. 18, p. 1023–1032.
- Avouac, J. P., and Burov, E. B., 1996, Erosion as a driving mechanism of intracontinental growth: *Journal of Geophysical Research*, v. 101, p. 17747–17769.
- Batt, G. E., and Braun, J., 1999, The tectonic evolution of the Southern Alps, New Zealand; insights from fully thermally coupled dynamical modeling: *Geophysical Journal International*, v. 136, p. 403–420.
- Beaumont, C., Fullsack, P., and Hamilton, J., 1992, Erosional control of active compressional orogens, in McClay, K. R., editor, *Thrust Tectonics*: New York, Chapman and Hall, p. 1–18.
- Beaumont, C., Ellis, S., Fullsack, P., and Hamilton, J., 1996, Mechanical model for subduction-collision tectonics of alpine-type compressional orogens: *Geology*, v. 24, p. 675–678.
- Bishop, M. P., and Shroder, J. F., Jr., 2000, Remote sensing and geomorphometric assessment of topographic complexity and erosional dynamics in the Nanga Parbat massif, in Khan, M. A., Treloar, P. J., Searle, M. P., and Jan, M. Q., editors, *Tectonics of the Nanga Parbat Syntaxis and the Western Himalaya*: London, Geological Society of London, Geological Society Special Publication 170, p. 180–200.
- Brace, W. F., and Kohlstedt, D. L., 1980, Limits on lithospheric stress imposed by laboratory experiments: *Journal of Geophysical Research*, v. 85, p. 6248–6252.
- Burbank, D. W., Leland, J., Fielding, E., Anderson, R. S., Brozovic, N., Reid, M. R., and Duncan, C., 1996, Bedrock incision, rock uplift, and threshold hillslopes in the northwestern Himalaya: *Nature*, v. 379, p. 505–510.
- Burg, J. P., and Podladchikov, Y., 1999, Lithospheric scale folding: numerical modeling and application to the Himalayan syntaxes: *International Journal Earth Sciences*, v. 88, p. 190–200.
- Burg, J. P., Davy, P., Nievergelt, P., Oberli, F., Seward, D., Diao, Z., and Meier, M., 1997, Exhumation during crustal folding in the Namche Barwa syntaxis: *Terra Nova*, v. 9, p. 117–123.

- Butler, R. W. H., Harris, N. B. W., and Whittington, A. G., 1997, Interactions between deformation, magmatism, and hydrothermal activity during crustal thickening: A field example from Nanga Parbat, Pakistan Himalaya: *Mineralogical Magazine*, v. 61, p. 37–51.
- Chamberlain, C. P., and Lyons, J. B., 1983, Pressure, temperature and metamorphic zonation studies of pelitic schists in the Merrimack synclinorium, south central New Hampshire: *American Mineralogist*, v. 68, p. 530–540.
- Chamberlain, C. P., Zeitler P. K., Barnett D. E., Winslow, D., Poulson, S. R., Leahy, T., and Hammer, J. E., 1995, Active hydrothermal systems during the recent uplift of Nanga Parbat, Pakistan Himalaya: *Journal of Geophysical Research*, v. 100, p. 439–453.
- Chamberlain, C. P., Koons, P. O., Meltzer, A. S., Craw, D., Zeitler, P. K., and Poage, M. A., 2002, Overview of hydrothermal activity associated with active orogenesis and metamorphism: Nanga Parbat, Pakistan Himalaya: *American Journal of Science*, v. 302, p. 726–748.
- Coward, M. P., and Butler, R. W. H., 1985, Thrust tectonics and the deep structure of the Pakistan Himalayas: *Geology*, v. 13, p. 417–420.
- Craw, D., Koons, P. O., Winslow, D., Chamberlain, C. P., and Zeitler, P. K., 1994, Boiling fluids in a region of rapid uplift, Nanga Parbat Massif, Pakistan: *Earth and Planetary Science Letters*, v. 128, p. 169–182.
- Craw, D., Chamberlain, C. P., Zeitler, P. K., and Koons, P. O., 1997, Geochemistry of a dry steam geothermal zone formed during rapid uplift of Nanga Parbat, northern Pakistan: *Chemical Geology*, v. 142, p. 11–22.
- Cundall, P. A., and Board, M., 1988, A microcomputer program for modeling large-strain plasticity problems, in Swododa, C., editor, *Numerical Methods in Geomechanics*, Proceedings 6th International Conference on Numerical Methods in Geomechanics, Innsbruck, Austria, April 11–15: Rotterdam, Balkema, p. 2101–2108.
- Davis, D., and Lillie, R. J., 1993, Changing mechanical response during continental collision: active examples from the foreland thrust belts of Pakistan: *Journal of Structural Geology*, v. 16, p. 21–34.
- Davis, D., Suppe, J., and Dahlen, F. A., 1983, Mechanics of fold-and-thrust belts and accretionary wedges: *Journal of Geophysical Research*, v. 88, p. 1153–1172.
- De Mets, C., Gorden, R. G., Argus, D. F., and Stein, S., 1990, Current plate motions: *Geophysical Journal*, v. 101, p. 425–478.
- Ellis, S., 1996, Forces driving continental collision: Reconciling indentation and mantle subduction tectonics: *Geology*, v. 24, p. 699–702.
- England, P., and Houseman, G., 1986, Finite strain calculations of continental deformation, 2. Comparison with the India-Asia collision zone: *Journal of Geophysical Research*, v. 91, p. 3664–3676.
- England, P., and Searle, M., 1986, The Cretaceous-Tertiary deformation of the Lhasa block and its implications for crustal thickening in Tibet: *Tectonics*, v. 5, p. 1–14.
- England, P. C., and Thompson, A. B., 1984, Pressure-temperature-time paths of regional metamorphism, Part I: Heat transfer during the evolution of regions of thickened continental crust: *Journal of Petrology*, v. 25, p. 894–928.
- Enlow, R. L., and Koons, P. O., 1998, Critical wedges in three dimensions; analytical expressions from Mohr-Coulomb constrained perturbation analysis: *Journal of Geophysical Research*, v. 103, p. 4897–4914.
- Evans, B., and Kohlstedt, D. L., 1995, Rheology of Rocks, in Ahrens, T.J., editor, *Rock Physics and Phase Relations: A Handbook of Physical Constants*: American Geophysical Union, AGU Reference Shelf 3, p. 148–165.
- Gansser, A., 1964, *Geology of the Himalaya*: New York, Wiley-Interscience, 289 p.
- Gazis, C. A., Blum, J. D., Chamberlain, C. P., and Poage, M., 1998, An isotopic study of granite genesis: Nanga-Parbat Haramosh Massif, Pakistan Himalaya: *American Journal of Science*, v. 298, p. 673–698.
- Hallet, B., and Molnar, P., 2001, Distorted drainage basins as markers of crustal strain east of the Himalaya: *Journal of Geophysical Research*, v. 106, p. 13,697–13,709.
- Hobbs, B. E., Muhlhaus, H. B., and Ord, A., 1990, Instability, softening, and localization of deformation, in Knipe, R. J., and Rutter, E. H., *Deformation mechanisms, rheology and tectonics*: London, Geological Society of London, Special Publication, v. 54, p. 143–165.
- Hochstein, M. P., and Yang, Z., 1992, Modelling of terrain-induced advective flow in Tibet: Implications for assessment of crustal heat flow: Stanford, California, Stanford 17th Annual Workshop on Reservoir Engineering.
- Hollister, L. S., and Crawford, M. L., 1986, Melt-enhanced deformation: A major tectonic process: *Geology*, v. 14, p. 558–561.
- Holt, W. E., 2000, Correlated crust and mantle strain fields in Tibet: *Geology*, v. 28, p. 67–70.
- Holt, W. E., Ming, L., and Haines, A. J., 1995, Earthquake strain rates and instantaneous relative motions within central and eastern Asia: *Geophysical Journal International*, v. 122, p. 569–593.
- Hubbert, M. K., and Rubey, W. W., 1959, Role of fluid pressure in mechanics of overthrust faulting, 1. Mechanics of fluid-filled porous solids and its application to overthrust faulting: *Geological Society of America Bulletin*, v. 70, p. 115–166.
- Jamieson, R. A., and Beaumont, C., 1988, Orogeny and metamorphism: A model for deformation and pressure-temperature-time paths with application to the central and southern Appalachians: *Tectonics*, v. 7, p. 417–446.
- Kidd, W. S. F., Edwards, M. A., Khan M. A., Schneider, D. A., Zeitler, P. K., Anastasio, D. A., Pecher, A., Le Fort, P., and Seeber, L., 1998, Structure and chronology of Nanga Parbat Haramosh massif: [abs]. *Eos Transactions, American Geophysical Union*, v. 79, p. 909.
- King, R. W., Shen, F., Burchfiel, B. C., Royden, L. H., Wang, E., Chen, Z., Liu, Y., Zhang, Z. Y., Zhao, J. Y., and Li, Y., 1997, Geodetic measurement of crustal motion in southwest China: *Geology*, v. 25, p. 179–182.

- Koons, P. O., 1987, Some thermal and mechanical consequences of rapid uplift: an example from the Southern Alps: *Earth and Planetary Science Letters*, v. 86, p. 307–319.
- 1990, The two sided wedge in orogeny; erosion and collision from the sand box to the Southern Alps, New Zealand: *Geology*, v. 18, p. 679–682.
- Koons, P. O., and Zeitler, P. K., 1997, Himalayan tectonics with a grain of salt: A view from the left-hand edge: *Eos: Transactions American Geophysical Union*, v. 78, p. S111.
- Koons, P. O., Craw, D., Cox, S., Upton, P., Templeton, A., and Chamberlain, C. P., 1998, Fluid flow during active oblique convergence: a Southern Alps model from mechanical and geochemical observations: *Geology*, v. 26, p. 159–162.
- Liu, L., and Zoback, M. D., 1992, The effect of topography on the state of the crust: Application to the site of the Cajon Pass Scientific Drilling Project: *Journal of Geophysical Research*, v. 97, p. 5095–5108.
- Maggi, A., Jackson, J. A., McKenzie, D., and Priestley, K., 2000, Earthquake focal depths, effective elastic thickness, and the strength of the continental lithosphere: *Geology*, v. 28, p. 495–498.
- McTigue, D. F., and Mei, C. C., 1981, Gravity-induced stresses near topography of small slope: *Journal of Geophysical Research*, v. 86, p. 9268–9278.
- Meltzer, A. S., Zeitler, P. K., Schoemann, M. L., Beaudoin, B. C., Seeber, L., and Armbruster, J. G., 1996, The Nanga Parbat seismic experiment, [abs.]: *American Geophysical Union, EOS: Transactions*, v. 77, p. F688.
- Meltzer, A., Sarker, G., Beaudoin, B., Seeber, L., and Armbruster, J., 2001, Seismic characterization of an active metamorphic massif, Nanga Parbat, Pakistan, Himalaya: *Geology*, v. 29, p. 651–654.
- Nelson, K. D., Zhao, W. J., Brown, L. D., Kuo, J., Che, J. K., Liu, X. W., Klemperer, S. L., Makovsky, Y., Meissner, R., Mechie, J., Kind, R., Wenzel, F., Ni, J., Nabelek, J., Chen, L. S., Tan, H. D., Wei, W. B., Jones, A. G., Booker, J., Unsworth, M., Kidd, W. S. F., Hauck, M., Alsdorf, D., Ross, A., Cogan, M., Wu, C. D., Sandvol, E., and Edwards, M., 1996, Partially molten middle crust beneath southern Tibet: Synthesis of project INDEPTH results: *Science*, v. 274, p. 1684–1688.
- Ord, A., and Oliver, N. H. S., 1997, Mechanical controls on fluid flow during regional metamorphism: Some numerical models: *Journal of Metamorphic Geology*, v. 15, p. 345–359.
- Panian, J., and Pilant, W., 1990, A possible theoretical explanation for foreland thrust propagation: *Journal of Geophysical Research*, v. 95, p. 8609–8615.
- Park, S. K., and Mackie, R. L., 1997, Crustal structure at Nanga Parbat, northern Pakistan, from magnetotelluric sounding: *Geophysical Research Letters*, v. 24, p. 2415–2418.
- 2000, Resistive (dry?) lower crust in an active orogen, Nanga Parbat, northern Pakistan: *Tectonophysics*, v. 316, p. 359–380.
- Patino-Douce, A. E., and Harris, N. B. W., 1998, Experimental constraints on Himalayan anatexis: *Journal of Petrology*, v. 39, p. 689–710.
- Pavlis, T. L., Hamburger, M. W., and Pavlis, G. L., 1997, Erosional processes as a control on the structural evolution of an actively deforming fold and thrust belt: An example from the Pamir-Tien Shan region, central Asia: *Tectonics*, v. 16, p. 810–822.
- Poage, M. A., Chamberlain, C. P., and Craw, D., 2000, Massif-wide metamorphism and fluid evolution at Nanga Parbat, northern Pakistan: *American Journal of Science*, v. 300, p. 463–482.
- Ramberg, H., 1973, Model studies of gravity controlled tectonics by the centrifuge technique, *in* DeJong, K., and Scholten, R., editors, *Gravity and Tectonics*: New York, John Wiley and Sons, p. 49–77.
- Ranalli, G., 1987, *Rheology Of The Earth: Deformation and flow processes in geophysics and geodynamics*: New York, Allen & Unwin Inc., 366 p.
- Rosenfeld, J. L., 1969, Rotated garnets in metamorphic rocks: *Geological Society of America, Special Paper* 129, 105 p.
- Royden, L. H., Burchfiel, B. C., King, R. W., Wang, E., Chen, Z., Shen, F., and Liu, Y., 1997, Surface deformation and lower crustal flow in eastern Tibet: *Science*, v. 276, p. 788–790.
- Sarker, G. L., Meltzer, A. S., Seeber, L., and Armbruster, J., 1999, Seismic attenuation and evidence of thermal anomalies beneath Nanga Parbat, western Himalaya [abs.]: *American Geophysical Union, Eos: Transactions*, v. 80, p. F722.
- Savage, W. Z., and Swolfs, H. S., 1986, Tectonic and gravitational stress in long symmetric ridges and valleys: *Journal of Geophysical Research*, v. 91, p. 3677–3685.
- Schneider, D. A., Edwards, M. A., Kidd, W. S. F., Khan, A., Seeber, L., and Zeitler, P. K., 1999a, Tectonics of Nanga Parbat, western Himalaya; synkinematic plutonism with doubly vergent shear zones of a crustal-scale pop-up structure: *Geology*, v. 27, p. 999–1002.
- Schneider, D. A., Edwards, M. A., Kidd, W. S. F., Zeitler, P. K., and Coath, C. D., 1999b, Early Miocene anatexis identified in the western syntaxis, Pakistan Himalaya: *Earth and Planetary Science Letters*, v. 167, p. 121–129.
- Seeber, L., Armbruster, J. G., and Quittmeyer, R. C., 1981, Seismicity and continental subduction in the Himalayan arc: *American Geophysical Union, Geodynamics Series* 3, p. 215–242.
- Shen, F., Royden, L. H., and Burchfiel, B. C., 2001, Large-scale crustal deformation of the Tibetan Plateau: *Journal of Geophysical Research*, v. 106, p. 6793–6816.
- Shroder, J. F., Jr., and Bishop, M. P., 2000, Unroofing of the Nanga Parbat Himalaya: *in* Khan, M. A., Treloar, P. J., Searle, M. P., and Jan, M. Q., editors, *Tectonics of the Nanga Parbat Syntaxis and the western Himalaya*: London, Geological Society of London, Special Publication 170, p. 163–179.
- Sonder, L. J., and England, P., 1986, Vertical averages of rheology of the continental lithosphere: Relation to thin sheet parameters: *Earth and Planetary Science Letters*, v. 77, p. 81–90.
- Terzaghi, K., 1943, *Theoretical Soil Mechanics*: New York, John Wiley, 510 p.
- Upton, P., 1998, Modelling localisation of deformation and fluid flow in a compressional orogen: Implications for the Southern Alps of New Zealand: *American Journal of Science*, v. 289, p. 296–323.

- Upton, P., Koons, P. O., and Chamberlain, C. P., 1995, Penetration of deformation-driven meteoric water into ductile rocks: isotopic and model observations from the Southern Alps, New Zealand: *New Zealand Journal of Geology and Geophysics*, v. 38, p. 535–543.
- Whittington, A. G., Harris, N. B. W., Ayres, M. W., and Foster, G., 2000, Tracing the origins of the western Himalaya: an isotopic comparison of the Nanga Parbat massif and Zaskar Himalaya, in Khan, M. A., Treloar, P. J., Searle, M. P., and Jan, M. Q., editors, *Tectonics of the Nanga Parbat Syntaxis and the Western Himalaya: Geological Society of America Special Publication 170*, p. 25–50.
- Willett, S. D., 1999, Orogeny and orography: The effects of erosion on the structure of mountain belts: *Journal of Geophysical Research*, v. 104, p. 28,957–28,982.
- Willett, S. D., Beaumont, C., and Fullsack, P., 1993, Mechanical model for the tectonics of doubly vergent compressional orogens: *Geology*, v. 21, p. 371–374.
- Winslow, D. M., Chamberlain, C. P., and Zeitler, P. K., 1995, Metamorphism and melting of the lithosphere due to rapid denudation, Nanga Parbat Massif, Himalaya: *Journal of Geology*, v. 103, p. 395–409.
- Zeitler, P. K., 1985, Cooling history of the northwest Himalaya, Pakistan: *Tectonics*, v. 4, p. 127–151.
- Zeitler, P. K., and Chamberlain, C. P., 1991, Petrogenetic and tectonic significance of young leucogranites from the northwestern Himalaya, Pakistan: *Tectonics*, v. 10, p. 729–741.
- Zeitler, P. K., Koons, P. O., Bishop, M. P., Chamberlain, C. P., Craw, D., Edwards, M. A., Hamidullah, S., Jan, M. Q., Khan, M. A., Khattak, M. U. K., Kidd, W. S. F., Mackie, R. L., Meltzer, A. S., Park, S. K., Pecher, A., Poage, M. A., Sarker, G., Schneider, D. A., Seeber, L., and Shroder, J. F., 2001a, Crustal reworking at Nanga Parbat, Pakistan: Metamorphic consequences of thermal-mechanical coupling facilitated by erosion: *Tectonics*, v. 20, p. 712–728.
- Zeitler, P. K., Meltzer, A. S., Koons, P. O., Craw, D., Hallet, B., Chamberlain, C. P., Kidd, W. S. F., Park, S. K., Seeber, L., Bishop, M. P., Shroder, J. F., 2001b, Erosion, Himalayan tectonics and the geomorphology of metamorphism: *GSA Today*, v. 11, p. 4–8.